FISEVIER

Contents lists available at ScienceDirect

# Journal of Biomechanics

journal homepage: www.elsevier.com/locate/jbiomech www.JBiomech.com



# Short communication

# Mapping the spatiotemporal evolution of solute transport in articular cartilage explants reveals how cartilage recovers fluid within the contact area during sliding



Brian T. Graham<sup>a</sup>, Axel C. Moore<sup>b</sup>, David L. Burris<sup>a,b</sup>, Christopher Price<sup>a,b,\*</sup>

#### ARTICLE INFO

Article history: Accepted 28 January 2018

Keywords:
Cartilage mechanics
Solute transport
Cartilage lubrication
Cartilage tribology
In situ cartilage imaging

#### ABSTRACT

The interstitial fluid within articular cartilage shields the matrix from mechanical stresses, reduces friction and wear, enables biochemical processes, and transports solutes into and out of the avascular extracellular matrix. The balanced competition between fluid exudation and recovery under load is thus critical to the mechanical and biological functions of the tissue. We recently discovered that sliding alone can induce rapid solute transport into buried cartilage contact areas via a phenomenon termed tribological rehydration. In this study, we use in situ confocal microscopy measurements to track the spatiotemporal propagation of a small neutral solute into the buried contact area to clarify the fluid mechanics underlying the tribological rehydration phenomenon. Sliding experiments were interrupted by periodic static loading to enable scanning of the entire contact area. Spatiotemporal patterns of solute transport combined with tribological data suggested pressure driven flow through the extracellular matrix from the contact periphery rather than into the surface via a fluid film. Interestingly, these testing interruptions also revealed dynamic, repeatable and history-independent fluid loss and recovery processes consistent with those observed in vivo. Unlike the migrating contact area, which preserves hydration by moving faster than interstitial fluid can flow, our results demonstrate that the stationary contact area can maintain and actively recover hydration through a dynamic competition between load-induced exudation and sliding-induced recovery. The results demonstrate that sliding contributes to the recovery of fluid and solutes by cartilage within the contact area while clarifying the means by which it occurs.

© 2018 Elsevier Ltd. All rights reserved.

## 1. Introduction

Articular cartilage is the load-bearing, avascular tissue responsible for the near-frictionless and wear-free movement of joints. Without a direct blood supply, chondrocytes within cartilage rely on diffusive and convective processes to exchange fluids, nutrients, waste products, and signaling molecules with the bathing synovial fluid (Evans and Quinn, 2006; Garcia et al., 2003). Mechanical loading and the relative surface motion inherent to joint articulation largely control these transport processes (Holmes et al., 1980; Marouda,s 1975, 1976; Mow et al., 1992).

As a biphasic material, cartilage consists of an extracellular matrix (ECM) whose interstitial space is filled with fluid (Holmes

et al., 1980). When cartilage is loaded in compression, the exudation of interstitial fluid helps carry cellular waste out of the tissue into the surrounding synovial fluid. However, the exudation process causes a time-dependent reduction in tissue thickness, stiffness, lubrication, and permeability to fresh nutrients (Ateshian, 2009; Holmes and Mow, 1990; Mow et al., 1980).

Significant attention has been devoted to elucidating how cartilage replenishes nutrient supplies following fluid exudation. Static and low frequency cyclic compression reduce solute diffusion by reducing matrix pore size and permeability (Maroudas et al., 1968). However, faster loading cycles, comparable to those associated with gait, can enhance solute transport into cartilage via a combination of advection and preferential entrapment of large solutes within consolidated interstitial spaces (DiDomenico et al., 2016; Zhang et al., 2007). Joint articulation also promotes fluid and solute recovery by intermittently exposing the 'dehydrated' cartilage surface directly to the synovial bath, permitting osmotic and diffusion-driven transport of fluid and solutes into the surface

<sup>&</sup>lt;sup>a</sup> Department of Mechanical Engineering, University of Delaware, Newark, DE, United States

b Department of Biomedical Engineering, University of Delaware, Newark, DE, United States

<sup>\*</sup> Corresponding author at: 161 Colburn Lab, University of Delaware, Newark, DE 19716, United States.

E-mail addresses: btgraham@udel.edu (B.T. Graham), axel@udel.edu (A.C. Moore), dlburris@udel.edu (D.L. Burris), cprice@udel.edu (C. Price).

(Ekholm, 1955; Maroudas et al., 1968). Additionally, the fluid mechanics of joint articulation (e.g. hydrodynamic pressure) have been implicated in fluid and solute recovery and transport processes in cartilage (Gleghorn and Bonassar, 2008; Graham et al., 2017; Hou et al., 1992; Ling 1974; Moore and Burris, 2016; Wright and Dowson, 1976). However, these potential tribological consequences on cartilage fluid and nutrient recovery have proven difficult to isolate experimentally, particularly in the MCA where osmotic swelling during intermittent bath exposure is presumed to prevail.

Recently, our group has used the convergent stationary contact area (cSCA) configuration (Fig. 1A) to study these hypothetical hydrodynamic effects while eliminating confounding effects from dynamic compression or contact migration (Graham et al., 2017; Moore and Burris, 2016). Estimates for physiological sliding speeds are ~100 mm/s (Hou et al., 1992; Mow, 1969) with contact pressures between 1 and 6 MPa during daily joint use (Park et al., 2008). In our previous papers we found that sliding under contact pressures near these values (60 mm/s under 0.25 MPa contact pressure) drove marked cartilage fluid and solute recovery, as measured by in situ compression and confocal imaging of solute accumulation. Although we have shown that this purely slidinginduced recovery phenomenon, termed tribological rehydration, restores hydration, thickness, load support, lubrication, and 'nutrition' following exudation, the mechanism(s) underlying this phenomenon remain uncertain. In this study, we used intermittent resting periods between sliding bouts to map (image) the spatiotemporal evolution of solute transport from the bath into the buried contact interface as a means to elucidate the flow fields associated with tribological rehydration. In the process, we also discovered that each bout of brief sliding reversed the exudation that accompanied each static 'imaging' period, preventing net loss of interstitial fluid or pressure over the long term. Given the intermittency inherent to human movement, we think this dynamic balance between exudation and tribological rehydration may provide important insight into the links between exercise and longterm joint health (Ageberg et al., 2012; Bosomworth, 2009; Hunter and Eckstein, 2009; Manninen, 2001; Rogers et al., 2002; Urquhart et al., 2011; Williams, 2013).

#### 2. Methods

#### 2.1. Setup design

19 mm diameter osteochondral cores were harvested from the femoral condyles of previously frozen mature bovine stifles, stained overnight in 10 µM 5'-DTAF (Life Technologies), and washed as described previously (Graham et al., 2017). Thawed sampled were tested within 4 days of harvesting, which has been previously shown to have no effect on tribological performance when compared to freshly harvested samples (Moore and Burris, 2015). Samples clamped via the subchondral bone were affixed to a mechanical tester featuring a linearly reciprocating glass slide that samples were compressed and slid against (Moore and Burris, 2016). This testing configuration (Fig. 1A) is classified as a convergent stationary contact area (cSCA), because a portion of the total cartilage surface area is in constant contact with the glass, thereby creating 'convergent wedges' at the contact periphery. The tester was mounted adjacent to an LSM880 confocal microscope used to image the buried cSCA contact during the sliding experiments using a 20x objective (LD Plan-Neofluar 20x/0.4, Carl Zeiss Microscopy) and light inverter.

## 2.2. Mechanical testing

Samples were preconditioned by applying 5 N compression, sliding at 60 mm/s, then free-swelling in 1X phosphate buffered saline (PBS), with each step lasting 2 min. The loading protocol shown in Fig. 1B begins with the initial application of a static 5 N load followed by alternating periods of reciprocal sliding (2 min) at 60 mm/s over a 20-mm distance (in both forward and reverse

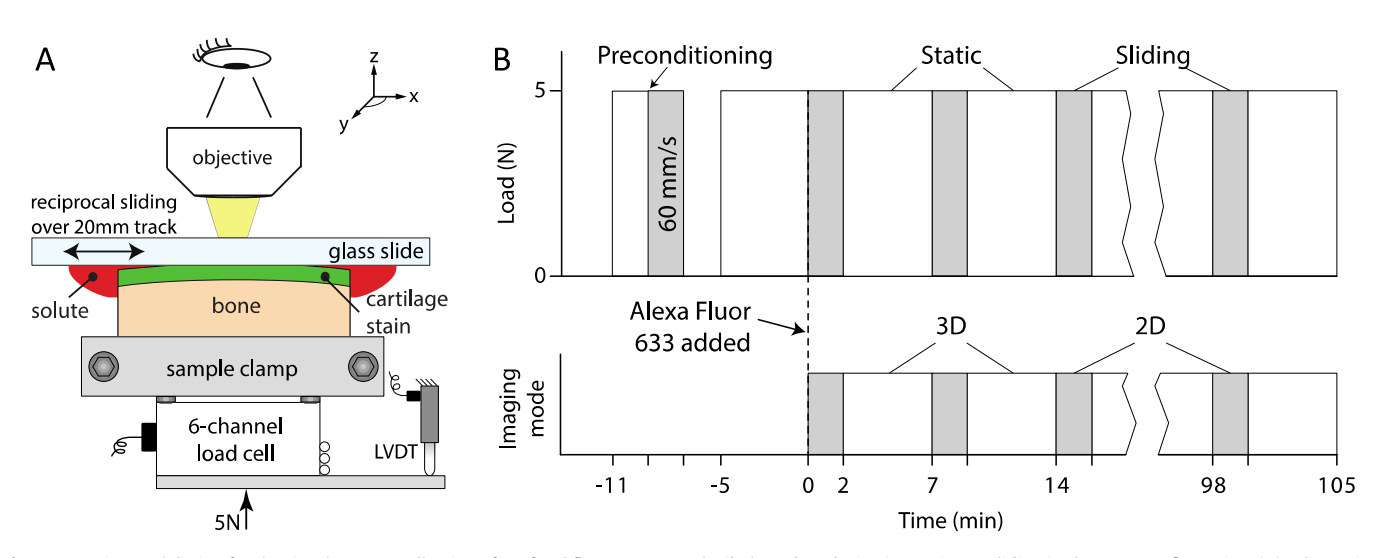


**Fig. 1.** Experimental design for the simultaneous collection of confocal fluorescence and tribology data during intermittent sliding in the cSCA configuration. (A) Schematic of the combined microscope and tribometer configuration. The sample remains stationary relative to the objective while the glass slide reciprocates, permitting simultaneous image and tribology data collection. The materials tester is mounted on an automated x-y stage to allow the generation of mosaic images of large areas, which is used to image the entire contact length. While the entire explant is not fully immersed in the solute solution, surface tension and adhesion to the glass cause the solution to fully envelope and bathe the cartilage. This condition is maintained even during high speed sliding. (B) Graphs depict the load applied to the sample along with the intermittent sliding and image capture conditions. Gray background indicates sliding at 60 mm/s while simultaneously collecting 2D time series of solute accumulation. White background indicates static contact while 'tiled' 3D scans were collected across the full contact length. A solution containing the small, neutral solute AlexaFluor 633 (AF633; shown in red) is used to replace the PBS bathing solution at time t = 0 min. (For interpretation of the references to colour in this figure legend, the reader is referred to the web version of this article.)

translations) and static contact (5 min). Just before initiating the first sliding bout, the PBS bath was replaced with 1 mL of small, neutrally charged fluorescent molecules (5  $\mu$ M AlexaFluor 633, 1.2 kDa, ThermoFisher Scientific) in PBS; resulting in the cartilage-on-glass contact being fully surrounded and covered by the solute solution during sliding (Fig. 1A).

#### 2.3. Imaging

During sliding periods, the confocal microscope was used to capture 2D time series at the center of contact in the plane (XZ)

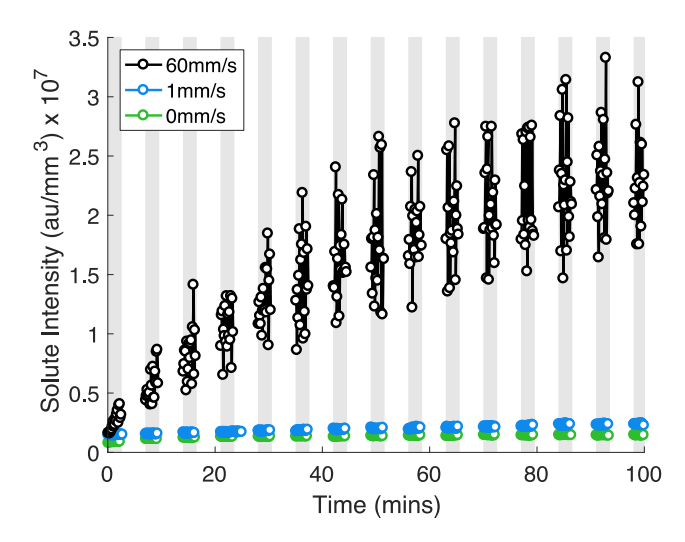


**Fig. 2.** Quantification of solute transport during intermittent sliding. Solute intensity in the 100- $\mu$ m thick by 425- $\mu$ m wide XZ plane (ROI) centered about the middle of the buried contact (R = 0.0) was summed for each frame in the image series and plotted as a function of time. Though the 60 mm/s reciprocal sliding generates noisy data, a monotonically increasing accumulation was observed at this speed, while negligible accumulation was observed at 0 and 1 mm/s. The overall trend of solute intensity change (accumulation) at all 3 speeds matches what had been found previously for continuously slid samples (Forster and Fisher 1996, 1999).

defined by the sliding and compression directions. During static contact intervals, 425- $\mu$ m wide 3D strips (XYZ) were captured in the sliding direction across the full length of the contact. In both cases, the 5-DTAF signal was used to locate the cartilage surface, measure the contact area, and isolate a 100- $\mu$ m tall region of interest (ROI) for solute accumulation analysis. Solute intensity was summed for each frame/tile and plotted as a function of normalized contact radius R\* = r/a, 'r' = radial position, and 'a' = contact radius. The image settings and the analysis methodologies are identical to those presented in our previous cSCA solute transport study (Graham et al., 2017).

#### 3. Results

#### 3.1. Solute transport

Solute intensity (accumulation) in the contact center (R\* = 0) during each 2-min sliding interval is shown as a function of time (sliding cycle) in Fig. 2. Despite the noise inherent to imaging during high speed sliding, the results suggest that solutes accumulated with a first-order time-dependence without obvious increases or decreases following static interruptions. Solute accumulation at each speed matched accumulation curves from continuous sliding experiments in prior work (Graham et al., 2017), demonstrating that intermittent static loading periods had negligible effects on the accumulation or distribution of solutes within the tissue.

Spatial solute accumulation profiles across the full contact length (collected during the 5 min static period) are shown qualitatively in Fig. 3 and Supplemental Videos 1–3, and quantitatively in Fig. 4A–C. When slid at 0 (static) or 1 mm/s, we observed no appreciable accumulation of florescence (comparable to the solute-free baseline) in the center of the contact, from  $-0.5 < R^{\ast} < 0.5$ ; solute only accumulated in regions immediately adjacent to the bathing solution, likely via free diffusion and solute trapping by the growing contact area (Fig. 3). In contrast, the 60 mm/s profiles showed large increases in red fluorescence in the center of the contact. The solute intensity gradients suggest transport from the convergent wedge towards the contact center.

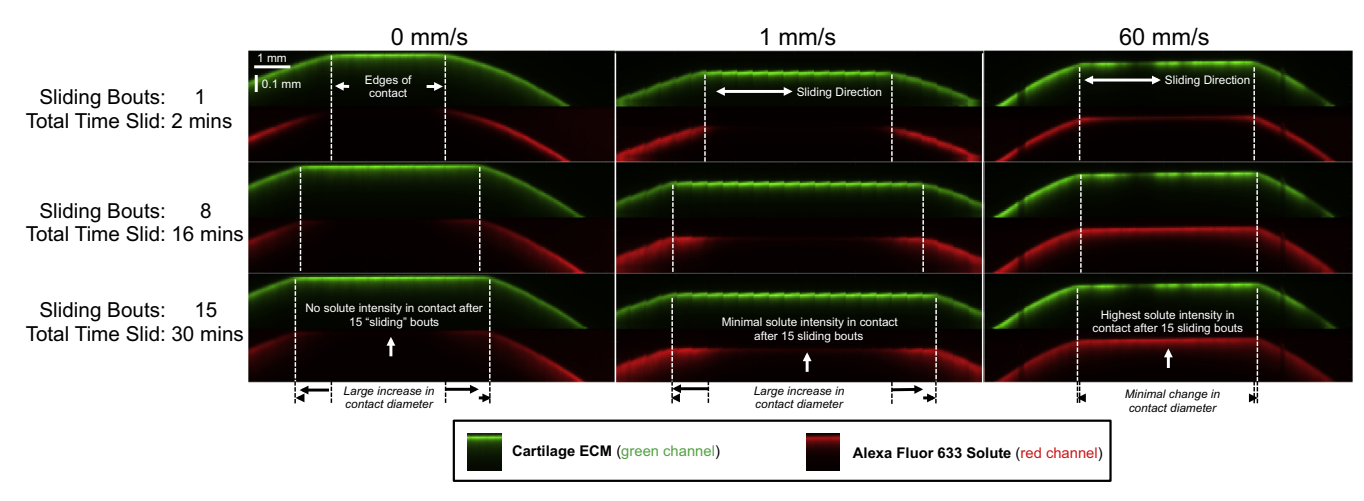
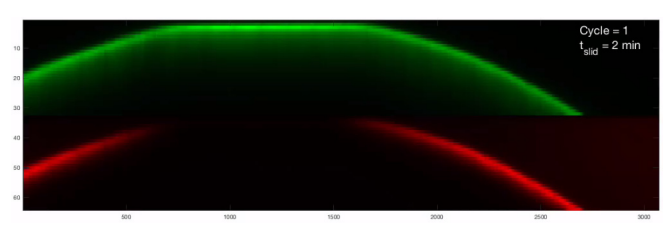
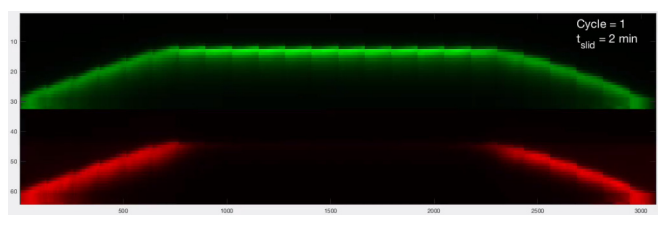


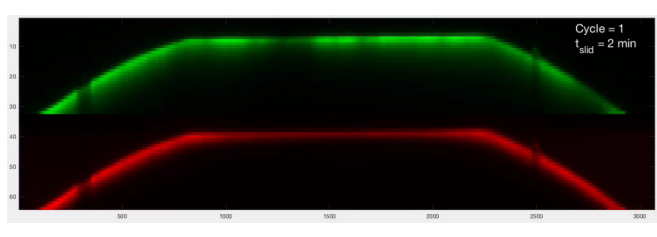
Fig. 3. Representative confocal images of sliding-induced solute transport into the cSCA buried contact. A different sample was tested for each speed. Images shown indicate solute accumulation after 1, 8, and 15 2-min. bouts of interrupted sliding for each test. The green channel represents the cartilage ECM and the red channel represents the solute (AlexaFluor 633) accumulated within the cartilage. The dashed lines indicate the edges of the contact area at each time point. At 0 and 1 mm/s the contact area expands as the sample continuously loses fluid and deforms against the glass, whereas the change in contact size is minimal in the 60 mm/s sample because high-speed sliding restores fluid and recovers deformation. Contact area increased by ~66, 49, and 13% for 0, 1, and 60 mm/s, respectively.



Supplemental Video 1.



Supplemental Video 2.



Supplemental Video 3.

# 3.2. Tribology

As shown in Fig. 5A, the deformation curves for sliding at 0 and 1 mm/s were nearly identical, with deformation increasing for the entire experiment. However, deformation in the 60 mm/s sample oscillated between upper and lower bounds, approaching a dynamic equilibrium during alternating sliding and rest. Additionally, friction dropped rapidly to  $\sim$ 0.02 during each bout of 60 mm/s sliding, while it remained at  $\sim$ 0.3 during sliding at 1 mm/s, a friction coefficient commonly cited as the equilibrium value for cartilage (Fig. 5B). Deformation and friction at the beginning and end of each sliding bout are plotted in Fig. 5C-D. Under 60 mm/s intermittent sliding, these deformation values delimit upper and lower strain envelopes that stabilize after 3-4 cycles, which suppressed cartilage strains over the long term. The friction coefficient, which was high immediately following static loading, decreased quickly, but not instantly, toward 0.02 without any obvious history dependence.

# 4. Discussion

While our previous study of the cSCA configuration demonstrated that sliding speed significantly influences solute accumulation in buried cartilage contacts, it only hinted at the mechanism by which this occurred (Graham et al., 2017). Here, breaking up the sliding into intervals allowed us to scan the entire contact area and reveal the spatiotemporal evolution of the solute accumulation during sliding. Once again, we saw that solute transport was speed dependent, with high speeds (60 mm/s) required to advect solutes into the center of the buried cartilage contact. Furthermore, the rate of advective transport was again orders of magnitude greater than that of diffusive transport in the absence of direct bath

exposure, reiterating the important role sliding likely plays in cartilage nutrition, particularly within the contact interface.

Previous studies have attributed low friction during high speed sliding to the formation of hydrodynamic fluid films. Had a fluid film formed, it is reasonable to expect at least some flow of that fluid film into the porous cartilage surface. In fact, Gleghorn and Bonassar proposed that efflux of fluid from the cartilage-glass interface into the tissue may have prevented them from achieving low friction from full-film lubrication (Gleghorn and Bonassar, 2008). The results of this study provide direct experimental insights into the fluid mechanics of this hypothetical situation. The solute concentration gradients in Fig. 4C provide clear evidence that solutes were advected from the leading edge of contact, rather than axially from a fluid film at the contact interface. Additionally, rehydration and solute accumulation were high even at the highest friction conditions (at the onset of sliding), which indicates that rehydration preceded any eventual fluid film formation. Both results suggest that hydrodynamic pressure at the leading edge of contact (wedge tip) pumped fluid and solutes directly into the adjacent cartilage surface rather than between the surfaces; propagation of this rehydration front across the contact is consistent with the observed solute concentration gradient (Fig. 4C) and the gradually decreasing friction coefficients following static loading (Fig. 5B).

An equally interesting and unanticipated result of this study was the deformation response to intermittent sliding (Fig. 5A). The sample exuded fluid as expected during each 5 min static loading period and recovered fluid during each 2 min bout of highspeed sliding. After an initial transient, the system achieved a dynamic equilibrium at  $\sim$ 220 µm of compression. Though sample thickness was not measured, this compression is approximately equal to ~21% strain based on measurements of similarly procured samples. Intermittent sliding not only disrupted the exudation process over the long-term, it mitigated the short-term loss of interstitial fluid, pressure, and lubrication. One could imagine that longer intervals of static loading between proportionally longer sliding bouts would cause greater exudation, reduced interstitial pressure. and greater shear stresses at the onset of sliding, each of which favors matrix degradation. These data suggest that the frequency of sliding may play a critical role in ensuring cartilage strains stay within a "safe" or "healthy" range (Carter et al., 2004; Guilak et al., 1994; Párraga Quiroga et al., 2016; de Vries et al., 2014). While it is unclear how tribological rehydration contributes to the recovery of fluid and solutes in vivo, these results may ultimately provide important mechanistic insights into the established link between joint disease and prolonged inactivity. We intend to explore these relationships in greater detail in future studies.

This study had a number of limitations worth noting. Firstly, while the use of cartilage-on-glass is non-physiological, it was necessary to permit in situ imaging and to eliminate osmotic swelling from intermittent bath exposure in the MCA (Caligaris and Ateshian, 2008; Krishnan et al., 2005). As long as cartilage-oncartilage contacts provide an appropriate hydrodynamic environment, we anticipate a similar fluid and solute recovery response for each surface. Secondly, we have only used a small neutral solute to date; this solute was chosen as a proxy for fluid flow, and given the advective nature of our hypothesis, we anticipate that tribological rehydration may be even more important for transporting larger solutes into cartilage (DiDomenico et al., 2016; Zhang et al., 2007). Thirdly, the tests performed were limited to sub-physiological pressures due to load limitations on the microscope slide. It is possible, if not likely, that hydrodynamic pressures become less competitive as interstitial pressures increase toward those found in vivo. Finally, the solute solution was aqueous whereas synovial fluid in the joint has a much higher viscosity. This has the potential to alter the transport of solutes

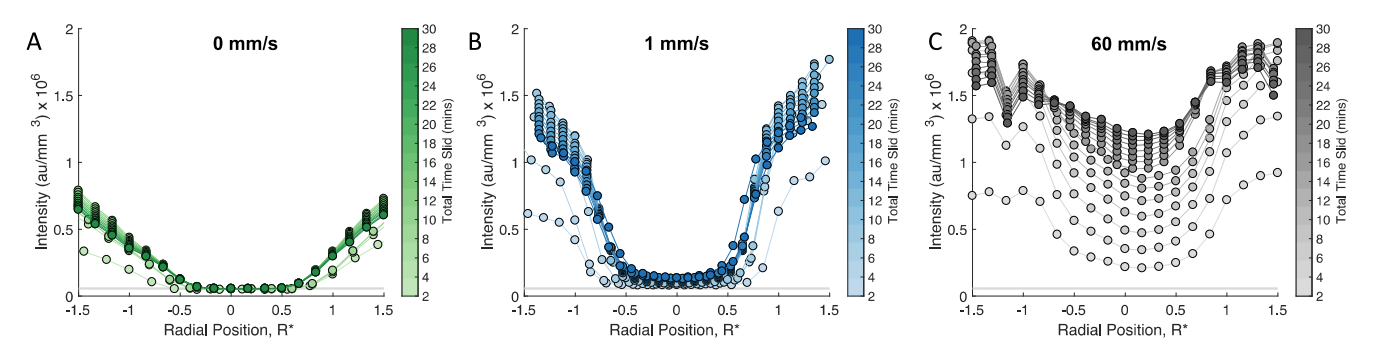
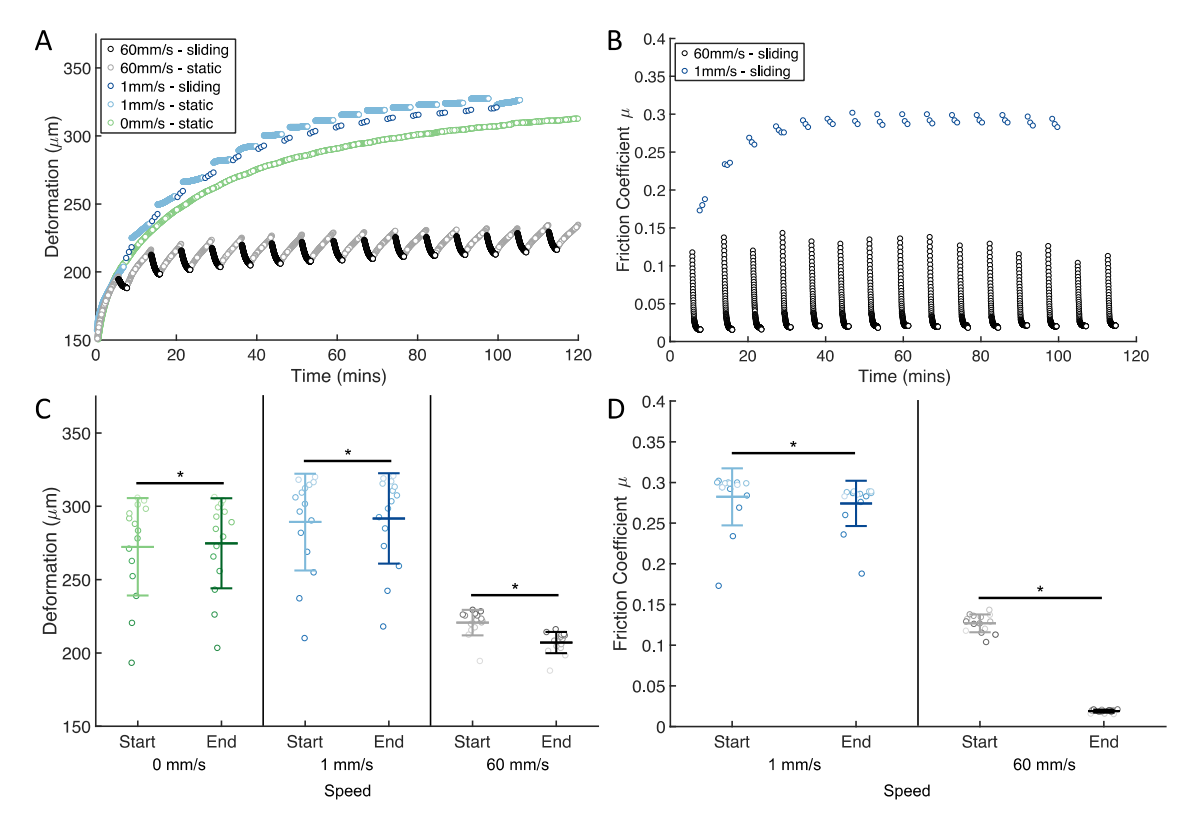


Fig. 4. Spatiotemporal quantification of sliding-induced solute transport into the cSCA buried contact in the direction of sliding. The x axis shows the normalized radial position for which the fluorescent intensity in the ROI of each cartilage subvolume was summed for 3 different sliding speed tests; (A) 0 mm/s, (B) 1 mm/s, and (C) 60 mm/s. The edges of contact are denoted at  $R^* = \pm 1$  and the center of contact is at  $R^* = 0$ . The gray bar just above the x axis represents the range of  $\pm$  one standard deviation from the mean of the baseline solute channel noise level in control samples imaged without any solute present. Markers are colored based on the total time lapsed during the experiment. The change in the spatial profiles over time at 60 mm/s suggest that solutes are driven in from the wedge and propagate through the contact with continued sliding.



**Fig. 5.** Tribological data collected during intermittent sliding experiments. (A) Deformation traces for a single sample at each sliding speed, with darker shaded symbols indicating when the sample experienced sliding. (B) Friction traces for the same samples slid at 1 or 60 mm/s. Change between (C) deformation and (D) friction values from the start of each individual 2 min sliding cycle to the end of that sliding cycle for the individual 0, 1, and 60-mm/s samples shown in A and B. There are 15 start and 15 end values for each sample, represented by the jittered-scatter of points behind the bars. The horizontal lines represent the mean and standard deviation of those scatter plots. The shading of the scatter point within each sample increases with cycle number in the same manner as Fig. 3. A paired *t*-test was performed within each sample, between the start and end values. indicates, on average, a significant difference between the start and end values for each speed (p < 0.05). Over the 2 min sliding bouts, cartilage strain and friction values were significantly reduced by sliding at 60 mm/s. Conversely, when cartilage was slid at 1 mm/s, deformation increased significantly over the 2 min bouts, while reductions in friction coefficients changes were much smaller (both are negative outcomes).

into the contact and is already known to reduce equilibrium friction coefficients in the cSCA configuration (Moore, 2017). Each of these is an active area of research to be addressed in future papers.

In summary, this study elucidated how sliding likely contributes, along with migration, osmotic swelling, and variable loading, to the retention and recovery of fluid and solutes by cartilage. Hydrodynamic pressure is the likely driving force underlying tribological rehydration and fluid and solutes appear to flow from the leading edge of contact into the tissue and across the interface,

rather than axially from a fluid film. Finally, the intermittent nature of the experiment demonstrated that regular sliding (articulation) can directly modulate the nutritional, mechanical, tribological, and presumably, the biochemical functions of articular cartilage. While these results cannot be directly extrapolated to the in vivo situation without further investigation, they provide an interesting mechanistic insight into the established link between regular exercise and overall joint health (Newton et al., 1997; Vanwanseele et al., 2002; Williams, 2013).

#### Conflict of interest statement

The authors have no competing interests to disclose.

## Acknowledgments

The authors thank Dr. Jeffrey Caplan and Michael Moore of the Biolmaging Center at the Delaware Biotechnology Institute for their technical assistance in setting up the experiments. Funding to study the mechanics of sliding-induced transport in articular cartilage was provided by the NSF Biomaterials and Mechanobiology Program under award number BMMB-1635536. Funding for the shared equipment and facilities at the DBI Biolmaging Center that were used in this research were provided by the NIH under award number S10 OD016361 and the Delaware INBRE program award number P20 GM103446. The content is solely the responsibility of the authors and does not necessarily represent the official views of the NSF, NIH, or INBRE.

#### **Author Contributions**

BTG, ACM, DLB, and CP all shared the discovery described, the research design, data analysis and manuscript writing.

#### References

- Ageberg, Eva et al., 2012. Effect of leisure time physical activity on severe knee or hip osteoarthritis leading to total joint replacement: a population-based prospective cohort study. BMC Musculoskeletal Disorders 13 (1), 73.
- Ateshian, Gerard A. 2009. "The Role of Interstitial Fluid Pressurization in Articular Cartilage Lubrication." 42:1163–76.
- Bosomworth, Neil J., 2009. Exercise and knee osteoarthritis: benefit or hazard? Canadian Family Physician 55 (9), 871–878.
- Caligaris, M., Ateshian, Gerard A., 2008. Effects of sustained interstitial fluid pressurization under migrating contact area, and boundary lubrication by synovial fluid, on cartilage friction. Osteoarthritis Cartilage 16, 1220–1227.
- Carter, Dennis R. et al., 2004. The mechanobiology of articular cartilage development and degeneration. Clin. Orthopaedics Related Res. 427, S69–S77.
- DiDomenico, Chris D., Wang, Zhen Xiang, Bonassar, Lawrence J., 2016. Cyclic mechanical loading enhances transport of antibodies into articular cartilage. J. Biomech. Eng. 139 (1). 11012-011012-17.
- Ekholm, Ragnar, 1955. Nutrition of articular cartilage. Acta Anatomy 24 (24), 329–338.
- Evans, Robin C., Quinn, Thomas M., 2006. Dynamic compression augments interstitial transport of a glucose-like solute in articular cartilage. Biophysical J. 91 (4), 1541–1547.
- Forster, H., Fisher, J., 1996. The influence of loading time and lubricant on the friction of articular cartilage. Proc. Inst. Mech. Eng., Part H: J. Eng. Med. 1989-1996 (vols 203-210) 210 (28), 109–119.
- Forster, H., Fisher, J., 1999. The influence of continuous sliding and subsequent surface wear on the friction of articular cartilage. Proc. Inst. Mech. Eng., Part H: J. Eng. Med. 213 (4), 329–345.
- Garcia, A. Minerva et al., 2003. Transport and binding of insulin-like growth factor I through articular cartilage. Arch. Biochem. Biophys. 415 (1), 69–79.
- Gleghorn, Jason P., Bonassar, Lawrence J., 2008. Lubrication mode analysis of articular cartilage using stribeck surfaces. J. Biomech. 41 (9), 1910–1918.
- Graham, Brian T., Moore, Axel C., Burris, David L., Price, Christopher, 2017. Sliding enhances fluid and solute transport into buried articular cartilage contacts. Osteoarthritis Cartilage, 1–8.
- Guilak, Farshid, Christoph Meyer, B., Ratcliffe, Anthony, Mow, Van C., 1994. The effects of matrix compression on proteoglycan metabolism in articular cartilage explants. Osteoarthritis Cartilage 2 (2), 91–101.

- Holmes, M.H., Mow, Van C., 1990. The nonlinear characteristics of soft gels and hydrated connective tissus in ultrafiltration. J. Biomech. 23 (11), 1145–1156.
- Holmes, M.H., Van C. Mow, Lai, W.M., 1980. "Fluid Transport and Mechanical Properties of Articular Cartilage: A Review".
- Hou, J.S., Mow, Van C., Lai, W.M., Holmes, M.H., 1992. An analysis of the squeezefilm lubrication mechanism for articular cartilage. J. Biomech. 25 (3), 247–259.
- Hunter, David J., Eckstein, Felix, 2009. Exercise and osteoarthritis. J. Anatomy 214 (2), 197–207.
- Krishnan, Ramaswamy, Mariner, Elise N., Ateshian, Gerard A., 2005. Effect of dynamic loading on the frictional response of bovine articular cartilage. J. Biomech. 38 (8), 1665–1673.
- Ling, F.F., 1974. A new model of articular cartilage in human joints. J. Lubricat. Technol. 96 (3), 449.
- Manninen, P., 2001. Physical exercise and risk of severe knee osteoarthritis requiring arthroplasty. Rheumatology 40 (4), 432–437.
- Maroudas, Alice, 1975. Fluid transport in cartilage. Ann. Rheumatic Diseases 34 Suppl 2 (Suppl), 77–81.
- Maroudas, Alice, 1976. Transport of solutes through cartilage: permeability to large molecules. J. Anatomy 122 (Pt 2), 335–347.
- Maroudas, Alice, Bullough, P., Swanson, S.A.V., Freeman, M.A.R., 1968. The permeability of articular cartilage. J. Bone Joint Surg., 166–177
- Moore, Axel C., 2017. Independent and Competing Roles of Fluid Exudation and Rehydration in Cartilage Mechanics and Tribology. University of Delaware. PhD thesis.
- Moore, Axel C., Burris, David L., 2015. Tribological and material properties for cartilage of and throughout the bovine stifle: support for the altered joint kinematics hypothesis of osteoarthritis. Osteoarthritis Cartilage 23 (1), 161–160
- Moore, Axel C., Burris, David L., 2016. Tribological rehydration of cartilage and its potential role in preserving joint health. Osteoarthritis Cartilage 25 (1), 1–9.
- Mow, Van C., 1969. The role of lubrication in biomechanical joints. J. Lubricat. Technol. 91 (2), 320.
- Mow, Van, C., Kuei, S.C., Lai, W.M., Armstrong, C.G., 1980. Biphasic creep and stress relaxation of articular cartilage in compression: theory and experiments. J. Biomech. Eng. 102 (1), 73–84.
- Mow, Van C., Ratcliffe, Anthony, Poole, A.R., 1992. Cartilage and diarthrodial joints as paradigms for hierarchical materials and structures. Biomaterials 13 (2), 67–
- Newton, P.M., Mow, Van C., Gardner, T.R., Buckwalter, J.A., Albright, J.P., 1997. The effect of lifelong exercise on canine articular cartilage. Am. J. Sports Med. 25 (3), 282–287
- Park, Seonghun, Nicoll, Steven B., Mauck, Robert L., Ateshian, Gerard A., 2008. Cartilage mechanical response under dynamic compression at physiological stress levels following collagenase digestion. Ann. Biomed. Eng. 36 (3), 425–424.
- Párraga Quiroga, J.M., Wilson, W., Ito, K., van Donkelaar, C.C., 2016. The effect of loading rate on the development of early damage in articular cartilage. Biomech. Model. Mechanobiol. 16 (1), 1–11.
- Rogers, L.Q., Macera, C.a., Hootman, J.M., Ainsworth, Be, Blair, S.N., 2002. The association between joint stress from physical activity and self-reported osteoarthritis: an analysis of the cooper clinic data. Osteoarthritis Cartilage 10, 617–622.
- Urquhart, Donna M. et al., 2011. What is the effect of physical activity on the knee joint? A systematic review. Med. Sci. Sports Exercise 43 (3), 432–442.
- Vanwanseele, B., Lucchinetti, E., Stüssi, E., 2002. The effects of immobilization on the characteristics of articular cartilage: current concepts and future directions. Osteoarthritis and Cartilage 10 (5), 408–419.
- de Vries, Stefan A.H. et al., 2014. Deformation thresholds for chondrocyte death and the protective effect of the pericellular matrix. Tissue Eng. Part A 20 (13–14), 1870–1876.
- Williams, Paul T., 2013. Effects of running and walking on osteoarthritis and hip replacement risk. Med. Sci. Sports Exercise 45 (7), 1292–1297.
- Wright, V., Dowson, Duncan, 1976. Lubrication and cartilage. J. Anatomy 121 (Pt 1), 107–118.
- Zhang, Lihai, Gardiner, Bruce S., Smith, David W., Pivonka, Peter, Grodzinsky, Alan J., 2007. The effect of cyclic deformation and solute binding on solute transport in cartilage. Arch. Biochem. Biophys. 457 (1), 47–56.